

# Meson-photon transition form factors and resonance cross-sections in $e^+e^-$ collisions

G. A. Schuler<sup>a,b</sup>, F. A. Berends<sup>a,c</sup>, R. van Gulik<sup>c</sup>

<sup>a</sup> *Theory Division, CERN, CH-1211 Geneva 23, Switzerland*

<sup>c</sup> *Instituut-Lorentz, University of Leiden, The Netherlands*

## Abstract

Meson-photon-photon transition form factors for  $S$ -,  $P$ -, and  $D$ -wave states are calculated, the meson being treated as a non-relativistic heavy-quark-antiquark pair. The full dependence on both photon virtualities is included. Cross-section formulas for charge-conjugation even mesons with  $J^P = 0^-, 0^+, 1^+, 2^+$ , and  $2^-$  in electron-positron collisions are presented and numerical results for LEP energies are given. In particular, we find two-photon event rates for  $\chi_{c1}$ ,  $\eta_c(2S)$ , and  $\eta_b(1S)$  within reach of LEP.

With minor modifications to incorporate  $SU(3)$ -flavour breaking we estimate rates for 18 light mesons as well, based on the observation that their two-photon decay widths agree remarkably well with measured data. Finally we point out that  $e^+e^-$  cross sections for  $1^+$  states do not vanish at low  $Q^2$ , the Landau-Yang suppression factors of the two-photon cross sections being compensated by the photon propagators.

---

<sup>b</sup> Heisenberg Fellow.

# 1 Introduction

In this paper we discuss resonance production in two-photon fusion in high-energy electron-positron ( $e^+e^-$ ) collisions. The main focus of our study is the dependence of the cross section on the photon virtualities  $Q_i^2$ , which we take fully into account. While there exist several papers on the  $Q^2$  dependence of the (single) form factor that governs the production of pseudo-scalar mesons [1, 2, 3, 4], much less is known about the (in general several) form factors associated with any other charge-conjugation even ( $C = +1$ ) meson [5, 6, 7] (for experimental data, see [8, 9]).

Here we present analytical results for the form factors and cross sections of  $C = +1$  mesons up to and including  $D$ -wave states. We compare these results with existing calculations where available. Moreover, we give numerical results for 30 mesons at typical LEP energies, for various representative experimental setups. All formulas are implemented in the Monte Carlo event generator GALUGA [10], and hence cross sections and distributions for any kind of  $e^+e^-$  environment can be easily obtained.

Let us now briefly discuss the theoretical framework in which our results are derived. Our calculation starts from the limit of heavy quarks, in which case a meson can be considered a non-relativistic bound state of a heavy quark ( $Q$ ) and a heavy antiquark ( $\bar{Q}$ ). Corrections from both the motion of the heavy quarks within the meson and higher-Fock-state components are small. The theoretical description of production and decay of heavy quarkonia is based on the NRQCD factorization framework [11], where relativistic corrections and higher-Fock-state contributions are suppressed by powers of  $v$ , the relative velocity of the quarks in the meson.

The velocity  $v$  is reasonably small for charmonia and bottomonia,  $\langle v^2 \rangle \sim 0.3$  and  $0.1$ , respectively, so that reliable results can be expected for heavy quarkonia. On the contrary, the application of this approach to light mesons (consisting of  $u$ ,  $d$ , and  $s$  quarks) can certainly not be derived from QCD and has to be considered as a model. However, we shall see that, with only minor modifications, the two-photon widths of essentially all measured light mesons agree remarkably well with data. Hence we proceed to present form factors and cross sections for the light mesons as well.

The dominant contribution to two-photon production of mesons arises from the (exclusive) short-distance process where a  $Q\bar{Q}$  pair is produced with quantum numbers equal to those of the asymptotic meson, i.e. where the meson is produced in its dominant Fock state. For a meson with total angular momentum  $J$ , parity  $P$  and charge-conjugation  $C$  this is a colour-singlet  $Q\bar{Q}$  pair with total spin  $S$  ( $= 0, 1$ ) and orbital angular momentum  $L$  ( $= 0, 1, 2, \dots$  or  $S, P, D$ , etc.) such that  $\mathbf{J} = \mathbf{L} + \mathbf{S}$ ,  $P = (-1)^{L+1}$  and  $C = (-1)^{L+S}$ . Specifically, for the five  $C = +1$  mesons of  $J^P = 0^-, J^+, 2^-$  considered in this paper, the dominant Fock state is a  $Q\bar{Q}$  state with  ${}^{2S+1}L_J = {}^1S_0, {}^3P_J, {}^1D_2$ , respectively (in the spectroscopic notation and  $J = 0, 1, 2$ ).

Four of the above mesons are produced in two-photon fusion without any short-distance suppression. Hence no enhanced  $O(\alpha_s)$  and  $O(v^2)$  corrections can occur and estimates based on the lowest-order  $O(\alpha^2 \alpha_s^0)$  calculation should be reliable. The situation could be different for the  $1^+$  state. Its  $O(\alpha^2)$  cross section vanishes when both photons are real and is therefore suppressed by  $\sim \langle Q^2 \rangle / M^2$  (details will be given below). Hence, if the reaction is not totally exclusive, other processes can be important. The  $Q^2$  suppression of the exclusive process  $\gamma\gamma \rightarrow R$  then competes with the suppression by extra powers of  $\alpha_s(m)$  and/or  $v^2$  of inclusive resonance production, which, however, are finite at zero  $Q_i^2$ .

To leading order in  $\alpha_s$  and/or  $v$ , three different mechanisms for the inclusive resonance production can occur for real photons. First, the short-distance production of a  $Q\bar{Q}_1(^3P_1)$ . Here and in the following a subscript 1 (8) indicates a colour-singlet (colour-octet)  $Q\bar{Q}$  pair. This production proceeds via  $\gamma\gamma \rightarrow Q\bar{Q}_1(^3P_1) + gg$  or  $Q\bar{Q}_1(^3P_1) + Q\bar{Q}$  and is suppressed by  $\alpha_s^2 v^0$ . Secondly, there is the  $\alpha_s^0 v^4$ -suppressed mechanism where a  $Q\bar{Q}_1(^3P_{0,2})$  pair, produced at short distances, turns into the  $1^+$  state via a double  $E1$  transition. Both contributions are small with respect to a third mechanism that is suppressed merely by a power of  $\alpha_s(m)$ : a  $Q\bar{Q}_8(^3S_1)$  pair is produced, which then turns into a  $Q\bar{Q}_1(^3P_1)$  via a single  $E1$  transition. The power of  $v^2$  of the  $E1$  transition is compensated by the fact that  $S$ -wave production is favoured against  $P$ -wave production by  $1/v^2$ . Whether or not any of the above-mentioned processes is important depends on the experimental setup: all these mechanisms are characterized by the presence of at least one more pion. Here we assume that the experimentally selected events are truly single resonance states so that these contributions are absent.

In the following sections we shall discuss helicity amplitudes and widths for the decay of resonances (section 2), form factors for the production (section 3) and finally results for the production cross sections.

## 2 Two-photon decays

Consider now the decay of a  $C = +1$  resonance into two photons,  $R(P) \rightarrow \gamma^*(k_1) + \gamma^*(k_2)$ , and define  $W = \sqrt{P^2}$ ,  $K_i = \sqrt{k_i^2}$ ,  $\nu = k_1 \cdot k_2$ , and  $X = \nu^2 - K_1^2 K_2^2$ . While  $W$  equals the resonance mass  $M$  for the decay, the two variables may differ for the crossed reaction, when one wants to take into account the Breit–Wigner formula in the production. We calculate the decay amplitudes using standard techniques<sup>1</sup>. We prefer to calculate helicity amplitudes rather than invariant amplitudes, since the former are more convenient to implement (after crossing) for the  $e^+e^-$  cross section respecting the full  $Q^2$  dependence. The amplitudes are given in the resonance rest system. As spin direction for the resonance we take the photon momentum.

Our results for the independent helicity decay amplitudes  $A(\lambda_1, \lambda_2)$  are listed in Table 1 in units of  $c_l = \sqrt{3/M} e_Q^2 16 \pi \alpha R_{nl}^{(l)}(0) Y_{l0}(0, 0)/D^{l+1}$  where  $Y_{lm}(\theta, \phi)$  are the spherical harmonics,  $D = W^2/4 - m^2 - \nu$ . In NRQCD the resonance mass is twice the quark mass,  $M \approx 2m$ . Here,  $R_{nl}^{(l)}(0)$  is the  $l$ -th derivative of the radial wave function  $R_{nl}(r) = \psi_{nlm}(\mathbf{r})/Y_{lm}(\theta, \phi)$  of the bound state at  $r = 0$ . The photon helicities can take on the values  $\lambda_i = \pm 1, 0$ . The remaining helicity amplitudes can be obtained using the relations

$$A(\lambda_1, \lambda_2) = \eta_R A(-\lambda_1, -\lambda_2) \quad (1)$$

$$A(\lambda_1, \lambda_2) = (-1)^J A(\lambda_2, \lambda_1)|_{K_1 \leftrightarrow K_2} \quad , \quad (2)$$

where  $\eta_R = 1$  ( $-1$ ) for mesons of the “normal” (“abnormal”)  $J^P$  series  $J^P = 0^+, 1^-, 2^+, \dots$  ( $J^P = 0^-, 1^+, 2^-, \dots$ ).

Our amplitudes are normalized such that the two-photon decay width is given by

$$\Gamma^{\gamma\gamma}[J^P] = \frac{1}{2J+1} \frac{1}{32\pi M} \sum_{\lambda_1, \lambda_2 = \pm 1} |A(\lambda_1, \lambda_2)|^2 \quad . \quad (3)$$

---

<sup>1</sup>We modify the projection operators of [12] to conform to the convention  $\text{diag}(g_{\mu\nu}) = (+, - - -)$  and to include colour, and extend the rules to  $D$ -wave states.

$J^P$	$A(+ -)$	$A(+ +)$	$A(+ 0)$	$A(0 0)$	$\Gamma_{\gamma\gamma}$
$0^-$	0	$\sqrt{X}$	0	0	4
$0^+$	0	$\frac{2(X+\nu W^2)}{\sqrt{3}W}$	0	$\frac{-2}{\sqrt{3}} K_1 K_2 W$	144
$1^+$	0	$\frac{-\sqrt{2}\nu}{W} (K_1^2 - K_2^2)$	$\sqrt{2} K_2 (\nu - K_1^2)$	0	32
$2^+$	$2W\nu$	$\sqrt{\frac{2}{3}} \frac{\nu(K_1^2+K_2^2)+2K_1^2K_2^2}{W}$	$\sqrt{2} K_2 (\nu + K_1^2)$	$2\sqrt{\frac{2}{3}} W K_1 K_2$	192/5
$2^-$	0	$4 \frac{X^{3/2}}{M^2}$	0	0	64

Table 1: Decay amplitudes  $A(\lambda_1, \lambda_2)$  in units of  $c_l$  and two-photon decay width (reduced with  $\tilde{\Gamma}_{\gamma\gamma}$  for  $1^+$ ) in units of  $d_l$  (see text for the definition of  $c_l, d_l$ ).

The width formulas are also displayed in Table 1 and agree with the literature, see e.g. [13]. Here we have defined  $d_l = 3 e_Q^4 \alpha^2 |R_{nl}^{(l)}(0)|^2 / M^{2(l+1)}$ . In the case of the  $1^+$  meson the entry defines the reduced width<sup>2</sup>  $\tilde{\Gamma}_{\gamma\gamma}$ . This is the transverse–transverse two-photon width divided by a factor  $[(K_1^2 - K_2^2)/(2\nu)]^2$ , which shows that  $\Gamma_{\gamma\gamma}[1^P]$  is zero, in agreement with the Landau–Yang theorem.

Before presenting numerical results for the two-photon widths, we have to discuss the input parameters, namely the wave functions and the squared charge factor  $e_Q^2$  appearing in  $c_l$  and  $d_l$ . Obviously, the electric charge of the quark is  $e_Q = +2/3$  ( $-1/3$ ) for charmonia (bottomonia). Moreover, the wave functions for the heavy quarkonia can quite reliably be calculated by solving the Schrödinger equation with a phenomenological inter-quark potential. We take values from a recent potential-model calculation [15]. The results are valid in the large-mass limit, where the non-relativistic expansion makes sense.

For the light mesons we have to assume the constituent quark model to be still a good approximation. We start from a linear potential  $\propto \lambda r$ , in which case  $|R_{nS}(0)|^2 = 2\mu\lambda$  (independent of the radial quantum number  $n$ ),  $|R'_{1P}(0)|^2 = 0.268 (2\mu\lambda)^{5/3}$ ,  $|R''_{1D}(0)|^2 = 0.151 (2\mu\lambda)^{7/3}$ , where  $\mu$  is the reduced mass. Using canonical values for the string tension  $\lambda$  and constituent-quark masses, we take  $2\mu\lambda = 0.74 \text{ GeV}^3$ . In order to incorporate  $SU(3)$  breaking we multiply the above squared wave functions by  $r_M^{2l+1}$ ,  $r_M = M/\mu_0$ , where  $M$  is the meson mass and  $\mu_0$  a hadronic scale of about 1 GeV. We thus use the following values for  $R_{nl}^{(l)}(0)$ :

	Light mesons	Charmonia	Bottomonia	
$ R_{1S}(0) ^2 / \text{GeV}^3$	$0.074 r_M$	0.81	6.5	
$ R'_{1P}(0) ^2 / \text{GeV}^5$	$3.5 \times 10^{-3} r_M^3$	0.075	1.4	(4)
$ R''_{1D}(0) ^2 / \text{GeV}^7$	$0.35 \times 10^{-3} r_M^5$	0.015	0.64	
$ R_{2S}(0) ^2 / \text{GeV}^3$	$0.074 r_M$	0.53	3.2	

For the light mesons we also have to replace  $e_Q^2$  by the effective squared charge  $\langle e_q^2 \rangle$ , which depends on the mixing angle  $\theta$  characterizing the breaking of the  $SU(3)$ -flavour

<sup>2</sup>Our  $\tilde{\Gamma}_{\gamma\gamma}$  coincides with that of [14] and is one half that of [7].

$i \setminus j$	$I = 1$	$I = 0$	$(I = 0)'$	$c\bar{c}$	$b\bar{b}$
$0^-$	$\pi^0$	$\eta$	$\eta'$	$\eta_c(1S)$	$\eta_b(1S)$
$1^1S_0$	$\frac{7.74}{10^3}(\frac{7.74}{10^3})$	0.41(0.46)	6.1(4.2)	7.8(7.5)	0.46(—)
$0^+$	$a_0$	$f_0$	$f'_0$	$\chi_{c0}$	$\chi_{b0}$
$3P_0$	5.1(> 0.24)	0.72(0.56)	10.4(5.4)	2.5(4.0)	0.043(—)
$1^+$	$a_1$	$f_1$	$f'_1$	$\chi_{c1}$	$\chi_{b1}$
$3P_1$	0.90(—)	2.5(2.4)	0.10(—)	0.50(—)	0.92/10 <sup>2</sup> (—)
$2^+$	$a_2$	$f_2$	$f'_2$	$\chi_{c2}$	$\chi_{b2}$
$3P_2$	1.0(1.0)	3.0(2.4)	0.12(0.097)	0.28(0.37)	0.74/10 <sup>2</sup> (—)
$2^-$	$\pi_2$	$\eta_D$	$\eta'_D$	$\eta_{cD}$	$\eta_{bD}$
$1D_2$	1.3(1.35)	0.43(—)	5.0(—)	0.95/10 <sup>2</sup> (—)	0.74/10 <sup>4</sup> (—)
$0^-$	$\pi(2S)$	$\eta(2S)$	$\eta'(2S)$	$\eta_c(2S)$	$\eta_b(2S)$
$2^1S_0$	6.9(—)	2.3(—)	23.0(—)	3.5(—)	0.20(—)

Table 2: The  $\gamma\gamma$  widths of the resonances in keV (reduced width  $\tilde{\Gamma}_{\gamma\gamma}$  in the case of  $3P_1$ ). Central values of the experimental measurements (in parentheses) from PDG [16], except for the  $3P_1$ , which is from TPC/2 $\gamma$  [14].

symmetry:

$$\begin{aligned}
\langle e_q^2 \rangle = & \frac{1}{3\sqrt{2}} & \pi, a_0, a_1, a_2, \pi_2 \\
& \frac{1}{3\sqrt{6}} (\cos\theta - 2\sqrt{2}\sin\theta) & \eta, f_0, f'_1, f'_2, \eta_D \\
& \frac{2}{3\sqrt{3}} (\cos\theta + \frac{1}{2\sqrt{2}}\sin\theta) & \eta', f'_0, f_1, f_2, \eta'_D.
\end{aligned} \tag{5}$$

The incorporation of  $SU(3)$  breaking outlined above can be refined by including the effect of the centrifugal barrier. Parity allows the orbital angular momentum of the photons to be 0 for the  $J^+$  states, but requires at least 1 for the cases of  $0^-$  and  $2^-$ . In our calculation this suppression shows up<sup>3</sup> as the factor  $\epsilon_{\alpha\beta\mu\nu} k_1^\alpha k_2^\beta \epsilon_1^\mu \epsilon_2^\nu \propto \sqrt{X}$  and therefore implies an additional factor  $r_M^2$  ( $r_M^4$ ) for the  $0^-$  and  $2^-$  helicity amplitudes (decay widths). Effectively this changes the power of  $r_M$  in (4) into  $n(J^P)$ , where  $n(J^P) = 5, 3, 9$  for  $J^P = 0^-, J^+, 2^-$ . Hence the two-photon widths scale with the meson mass as  $M^3$  for  $0^-$  and  $2^-$  states, and as  $1/M$  for  $J^+$  states. This can be compared with the ‘‘conventional’’ approach, where also the  $J^+$  mesons are assumed to scale as  $M^3$  [17, 18].

Numerical results for the two-photon widths of the  $n = 1$  ( $n$  the radial quantum number) mesons with  $J^P = 0^-, J^+$ , and  $2^-$  are given in Table 2 for charmonia and bottomonia as well as for the light mesons with isospin  $I = 0, 1$ . The masses of the mesons are taken from the PDG, where known, and the others from a potential-model calculation

<sup>3</sup> The additional factor  $X/M^2$  visible in Table 1 for the  $1D_2$  state arises from  $k_1^\mu k_2^\nu \epsilon_{\mu\nu}(2, J_z)$  and is not counted as a threshold factor.

[18]. The latter are the  $\eta_b(9400)$ , and the  $D$ -wave states  $\eta_D(1680)$ ,  $\eta'_D(1890)$ ,  $\eta_{cD}(3840)$ , and  $\eta_{bD}(10150)$  (particle masses in parentheses). We have boldly taken  $a_0(983.5)$ ,  $f_0(980)$ , and  $f_0(1370)$  as the lowest-lying isoscalar despite their questionable status. Values for the first radial excitation are given as well, where we took  $\pi[2S](1300)$ ,  $\eta[2S](1295)$ ,  $\eta'[2S](1400)$ ,  $\eta_c[2S](3594)$ ,  $\eta_b[2S](9980)$ .

The only free parameters are the scale  $\mu_0$  and the mixing angles. We do not try to fit these. Rather we adjust  $\mu_0$  by the  $\pi^0$  decay width to  $\mu_0 = 0.96 \text{ GeV}$ . We determine the mixing angles of the pseudo-scalars and the tensor mesons from the quadratic mass formula  $\theta[0^-] = -11.5^\circ$ ,  $\theta[2^+] = 32^\circ$ . Lacking further information, we simply take  $\theta = 32^\circ$  for the other  $P$ -wave states as well and  $\theta = 0$  for the  $D$ -wave and  $n = 2$   $S$ -wave states. A look at Table 2 shows that we find surprisingly good agreement with the measured decay widths for practically all measured mesons<sup>4</sup>! This gives us confidence that the approach provides sensible results for the two-photon production of these mesons as well.

### 3 Form factors for two-photon production

The differential cross section for the reaction  $e^+e^- \rightarrow e^+e^-X$ , where the (hadronic) final state  $X$  is produced by  $\gamma\gamma$  fusion, can (to lowest order in QED) be expressed in terms<sup>5</sup> of the cross sections for  $\gamma^*(q_1) + \gamma^*(q_2) \rightarrow X$  via[20]

$$\frac{E_1 E_2 d^6\sigma}{d^3\mathbf{p}_1 d^3\mathbf{p}_2} = \sum_{A,B} \mathcal{L}_{AB} \sigma_{AB} . \quad (6)$$

Here  $\sigma_{AB}(W, Q_1, Q_2)$  denote the cross sections of transverse ( $A, B = T$ ) and longitudinal ( $A, B = S$ ) photons with momenta  $q_i$ , which depend merely on the hadronic mass  $W = \sqrt{m_X^2}$  and the virtualities of the two photons  $Q_i = \sqrt{-q_i^2}$ . Furthermore,  $p_i = (E_i, \mathbf{p}_i)$  are the momenta of the outgoing leptons, and  $\mathcal{L}_{AB}$  are (in QED fully) calculable virtual-photon flux factors, related to the photon-density matrices  $\rho_i^{\lambda_1, \lambda_2}$  ( $\lambda_i = \pm 1, 0$ ). For example, in the standard notation[20]:

$$\mathcal{L}_{TT} = \frac{\alpha^2}{16\pi^4 Q_1^2 Q_2^2} \frac{2\sqrt{X}}{s\sqrt{1-4m_e^2/s}} 4\rho_1^{++}\rho_2^{++} . \quad (7)$$

Adapting the standard definition of the two-photon helicity cross sections

$$\begin{aligned} \sigma_{TT} &= \frac{1}{4\sqrt{X}} [W(++ , ++ ) + W(+ - , + - )] , & \sigma_{SS} &= \frac{1}{2\sqrt{X}} W(00, 00) , \\ \sigma_{TS} &= \frac{1}{2\sqrt{X}} W(+0, +0) , & \sigma_{ST} &= \frac{1}{2\sqrt{X}} W(0+, 0+) , \end{aligned} \quad (8)$$

we find

$$W(\lambda_1, \lambda_2; \lambda_1, \lambda_2) = \pi \delta(P^2 - M^2) |M(\lambda_1, \lambda_2)|^2 . \quad (9)$$

The amplitudes  $M$  are the ones for the crossed reaction obtained by replacing  $K_i$  by  $iQ_i$  in the helicity amplitudes  $A$ . Note that relation (2) is changed into

$$M(\lambda_1, \lambda_2) = (-1)^{J-\lambda_1+\lambda_2} M(\lambda_2, \lambda_1)|_{K_1 \leftrightarrow K_2} . \quad (10)$$

<sup>4</sup>For an (incomplete) list of previous estimates of two-photon widths see [17, 18, 19].

<sup>5</sup>We omit interference terms that integrate to zero over  $\tilde{\phi}$ , where  $\tilde{\phi}$  is the azimuthal separation between the two lepton planes in the  $\gamma^*\gamma^*$  cms.

$J^P$	$f_{TT}$	$f_{TS}$	$f_{SS}$
$0^-$	$\kappa \frac{X}{\nu^2}$	0	0
$0^+$	$\kappa \left( \frac{X + \nu M^2}{3\nu^2} \right)^2$	0	$2\kappa \left( \frac{M^2 \sqrt{Q_1^2 Q_2^2}}{3\nu^2} \right)^2$
$1^+$	$\kappa \left( \frac{Q_2^2 - Q_1^2}{2\nu} \right)^2$	$2\kappa \frac{M^2}{2\nu} \frac{Q_2^2}{2\nu} \left( \frac{\nu + Q_1^2}{\nu} \right)^2$	0
$2^+$	$\kappa \left( \frac{M^2}{2\nu} \right)^2 \left\{ 1 + \frac{[2Q_1^2 Q_2^2 - \nu(Q_1^2 + Q_2^2)]^2}{6M^4 \nu^2} \right\}$	$\kappa \frac{M^2 Q_2^2 (\nu - Q_1^2)^2}{4\nu^4}$	$\kappa \frac{M^4 Q_1^2 Q_2^2}{3\nu^4}$
$2^-$	$\kappa \left[ \frac{X}{\nu^2} \right]^3$	0	0

Table 3: Form factors  $f_{AB}$ .

We quote the final expression for the cross section for the production of the  $C = +1$  resonances in the form ( $A, B = T, S$ )

$$\sigma_{AB}[J^P] = \delta(W^2 - M^2) 8\pi^2 \frac{(2J+1)\Gamma_{\gamma\gamma}[J^P]}{M} f_{AB}[J^P]. \quad (11)$$

(For the  $1^+$  state we obviously use  $\tilde{\Gamma}$ .) The form factors  $f_{AB}$  are listed in Table 3, using the notation

$$\begin{aligned} \kappa &= \frac{M^2}{2\sqrt{X}} \quad \rightarrow 1 \quad \text{for both } Q_i^2 \rightarrow 0, \\ X &= \nu^2 - Q_1^2 Q_2^2, \quad \nu = \frac{1}{2} (W^2 + Q_1^2 + Q_2^2). \end{aligned} \quad (12)$$

Measurements of form factors for states other than the pseudo-scalar mesons are still very rough [8, 9, 14]. It is important to realize that the  $Q_i^2$  dependence of the form factors is convention-dependent. What is unique is the  $Q_i^2$  dependence of the  $e^+e^-$  cross section, but one is free to attribute terms that approach 1 for  $Q_i^2 \rightarrow 0$  to either the luminosity functions or the form factors governing the two-photon cross sections.

Conventions different from (11) are in use. Indeed, for the pseudo-scalar mesons  $P$  it has become standard to define the meson-photon transition form factor by writing the invariant amplitude as  $M[\gamma^*\gamma^* \rightarrow P(0^-)] = F_{P\gamma\gamma}(Q_i) e^2 i \epsilon_{\mu\nu\rho\sigma} q_1^\mu q_2^\nu \epsilon_1^\rho \epsilon_2^\sigma$ . In this convention the (only non-vanishing) two-photon cross section becomes

$$\sigma_{TT}[J^P] = \delta(W^2 - M^2) 8\pi^2 \frac{\Gamma_{\gamma\gamma}[J^P]}{M} \frac{1}{\kappa} \left[ \frac{F_{P\gamma\gamma}(Q_1, Q_2)}{F_{P\gamma\gamma}(0, 0)} \right]^2. \quad (13)$$

Hence  $F_{P\gamma\gamma}$  is related to our form factor by

$$\begin{aligned} \frac{F_{P\gamma\gamma}(Q_1, Q_2)}{F_{P\gamma\gamma}(0, 0)} &= \sqrt{\kappa f_{TT}[0^-]} = \frac{M^2}{M^2 + Q_1^2 + Q_2^2} = \frac{M^2}{2\nu}, \\ F_{P\gamma\gamma}(0, 0) &= \frac{4}{M} \sqrt{\frac{3e_Q^4 |R_{nS}(0)|^2}{\pi M^3}} = \frac{2}{M} \sqrt{\frac{\Gamma_{\gamma\gamma}}{\pi \alpha^2 M}} = \frac{4e_Q^2 f_P}{M^2}, \end{aligned} \quad (14)$$

where  $f_P$  is the pseudo-scalar decay constant,  $f_P = |R_S(0)|\sqrt{\frac{3}{\pi M}}$  for heavy mesons. Equation (14) agrees with a recent calculation [3] where also transverse-momentum ( $\mathbf{k}_T$ ) effects

of the quarks within the bound state were included. This effectively amounts to adding  $2\langle \mathbf{k}_T^2 \rangle$  to the denominator  $M^2 + Q_1^2 + Q_2^2$  in (14).

CLEO [21] has measured the single  $Q^2$  dependence ( $Q = Q_1, Q_2 \approx 0$ ) of the  $\pi^0$ ,  $\eta$ , and  $\eta'$  form factors very precisely. The data are consistent with a monopole behaviour with a pole mass close to the  $\rho$  mass for  $\pi^0$  and  $\eta$  and a slightly larger mass for  $\eta'$ . Our result (14) is indeed a monopole form factor, in agreement also with the power-counting rules [22]. We obtain good normalizations for the three pseudo-scalars, but the pole masses would be too small if we took the meson masses. On the other hand, these mesons being Goldstone bosons are exceptionally light. Therefore we take  $m_\rho$  ( $\approx$  twice the light quark mass) as pole mass for the three lightest pseudo-scalars, but identify the pole mass with the meson mass for all other mesons.

It is important to realize that  $F_{P\gamma\gamma}$  does not factorize into the product of two form factors  $F_R(Q_1^2) F_R(Q_2^2)$  as suggested by vector-meson dominance. There  $F_R(Q^2) = M_R^2/(M_R^2 + Q^2)$  with, for example,  $M_R = M_{J/\psi}$  for charmonia. In particular at large  $Q_1$  and  $Q_2$ , the form factor  $F_{P\gamma\gamma}$  is known to fall off only as  $M^2/(Q_1^2 + Q_2^2)$  [22, 23] rather than  $M^4/(Q_1^2 Q_2^2)$ .

At first sight it might seem to be a coincidence that we obtain the correct asymptotic behaviour, since our non-relativistic calculation becomes insufficient at asymptotic  $Q_i$  values where large logarithms  $\ln Q_i/M$  become important. Calculations with massive quarks in the non-relativistic approximation are well suited for  $Q_i$  values not much larger than the heavy-quark mass  $\sim M/2$ . At asymptotically large  $Q$ , it is more appropriate to set up a scheme in which calculations are done with massless quarks, but incorporating the  $Q^2$  evolution of the quark distribution amplitudes in the meson. Such an approach is provided by the hard-scattering approach (HSA) [1].

In the HSA, the meson–photon–photon transition amplitude factorizes into a hard (i.e. perturbatively calculable) scattering amplitude and a soft (i.e. long-distance) distribution amplitude (DA)  $\phi(x)$ , so that asymptotically

$$F_{P\gamma\gamma}(Q_1, Q_2) \rightarrow 2 \langle e_q^2 \rangle f_P \int_0^1 dx \frac{\phi(x)}{x Q_1^2 + (1-x) Q_2^2}. \quad (15)$$

Since all meson DAs approach the asymptotic form  $\phi_{\text{as}}(x) = 6x(1-x)$ , the asymptotic form of  $F_{P\gamma\gamma}$  is fully determined in QCD

$$\begin{aligned} F_{P\gamma\gamma} &\rightarrow 6 \langle e_q^2 \rangle f_P \frac{Q_1^4 - Q_2^4 - 2 Q_1^2 Q_2^2 \ln(Q_1^2/Q_2^2)}{(Q_1^2 - Q_2^2)^3} \\ &\rightarrow \frac{6 \langle e_q^2 \rangle f_P}{Q^2} \quad \text{for } Q_1 = Q, Q_2 = 0 \\ &\rightarrow \frac{2 \langle e_q^2 \rangle f_P}{Q^2} \quad \text{for } Q_1 = Q_2 = Q. \end{aligned} \quad (16)$$

Although the full  $Q_i$  dependence looks more complicated than (14), the two limiting cases show that the asymptotic power behaviours for large  $Q_1$  and/or large  $Q_2$  are identical. The reason is that in either calculation the hard vertex is  $Q\bar{Q}({}^1S_0) \rightarrow \gamma\gamma$  and asymptotically the HSA DA becomes  $Q$ -independent, as is the non-relativistic one. In fact, owing to the normalization condition  $\int dx \phi(x) = 1$ , the symmetric limit ( $Q_1 = Q_2$ ) is fully identical. The single asymptotic limit ( $Q_1 \rightarrow \infty, Q_2 = 0$ ) differs by a factor 2/3, reflecting the difference of the moment  $\langle 1/x \rangle = \int dx \phi(x)/x$  for the asymptotic DA and the non-relativistic DA,  $\phi_{\text{nr}} = \delta(x - 1/2)$ .



	$Q_1 \neq Q_2$			$Q_1 = Q_2 = Q$		
$J^P$	$F_{TT}$	$F_{TS}$	$F_{SS}$	$F_{TT}$	$F_{TS}$	$F_{SS}$
$0^-$	1	0	0	1	0	0
$0^+$	$\frac{\Delta}{3}$	0	$\frac{4\sqrt{2}M^2 Q_1 Q_2}{3\Delta(Q_1^2+Q_2^2)^2}$	$\frac{2M}{3Q}$	0	$\frac{\sqrt{2}M}{3Q}$
$1^+$	1	$\frac{\sqrt{2}M Q_2 (3Q_1^2+Q_2^2)}{\Delta(Q_1^2+Q_2^2)^2}$	0	0	$\sqrt{2}$	0
$2^+$	$\frac{\Delta}{\sqrt{6}}$	$\frac{M Q_2}{Q_1^2+Q_2^2}$	$\frac{4M^2 Q_1 Q_2}{\sqrt{3}\Delta(Q_1^2+Q_2^2)^2}$	$\frac{\sqrt{42}M}{12Q}$	$\frac{M^2}{4Q^2}$	$\frac{M}{\sqrt{3}Q}$
$2^-$	$\Delta^2$	0	0	$\frac{M^2}{Q^2}$	0	0

Table 4: Structure functions  $F_{AB}$ .  $\Delta = |Q_2^2 - Q_1^2|/(Q_2^2 + Q_1^2)$ .

Such numerical differences between our results and the HSA may also exist for the asymptotic behaviours of the other meson–photon transition form factors, which have not yet<sup>6</sup> been calculated in the HSA. However, we emphasize that the power fall-off is the same in the two approaches. Moreover, it is not clear at which  $Q_i$  values the asymptotic regime is reached. Eventually, one would like to match the massive-quark calculation at low  $Q_i$  with the HSA calculation at large  $Q_i$ .

The large- $Q_i$  behaviour of the form factors for the other  $J^P$  mesons is different from that of the pseudo-scalars. In analogy to  $F_{P\gamma\gamma}$  we define

$$F_{AB} = \lim_{Q_i \rightarrow \infty} \left[ \frac{Q_1^2 + Q_2^2}{M^2} \sqrt{\kappa f_{AB}} \right], \quad (17)$$

and give the results in Table 4. It can be seen that the double-asymptotic limit  $Q_i \rightarrow \infty$  in the symmetric case is different from the asymmetric limit. For  $Q_i \gg M$ , but  $Q_1 \neq Q_2$ , the  $F_{TT}$ 's are the dominant form factors; all other form factors are suppressed by powers of  $1/\max_i Q_i$ . On the contrary,  $F_{SS}[0^+]$  possesses the same power counting  $\propto 1/Q$  as  $F_{TT}[0^+]$  in the symmetric case. The same holds for  $2^+$  mesons, while  $F_{TT}[2^-]$  behaves as  $1/Q^2$  and Bose symmetry leads to a vanishing of  $F_{TT}[1^+]$ . In fact, besides  $F_{TT}[0^-]$  only  $F_{TS}[1^+]$  remains non-zero in the symmetric double-asymptotic limit. Therefore the cross sections for  $1^+$  mesons, which vanish at zero  $Q_i$ , become the largest  $P$ -wave cross sections at high  $Q_i$  in the symmetric limit.

Ideally the aim is to measure the dependence on both  $Q_1$  and  $Q_2$ , and to separate the form factors  $f_{SS}$ ,  $f_{TS}$ , and  $f_{TT}$  (as well as the latter in helicity-two and helicity-zero components). Obviously, such tasks require high statistics and excellent tagging efficiencies. Experimentally much more feasible are single-tag measurements,  $d\sigma/dQ_2^2$ . Often an anti-tag is imposed on the other electron in order to ensure  $Q_1 \approx 0$ . Such measurements are sensitive to only an effective form factor. We therefore generalize the pseudo-scalar form factor  $F_{P\gamma\gamma}$  and define

$$\left(F_{\text{eff}}(Q^2)\right)^2 = \lim_{Q_1^2 \rightarrow 0} \kappa [f_{TT} + \epsilon f_{TS}] \Big|_{Q_2^2=Q^2}, \quad (18)$$

<sup>6</sup>For a recent attempt to generalize the HSA to  $L \neq 0$  mesons, see [24].

where  $\epsilon$  is the ratio of the average luminosities  $\mathcal{L}_{TS}$  to  $\mathcal{L}_{TT}$ . Experimentally,  $\epsilon$  is often close to 1. We find:

$$\begin{aligned}
F_{\text{eff}}[0^-] &= \frac{M^2}{M^2 + Q^2} \\
F_{\text{eff}}[0^+] &= \frac{1}{3} \frac{M^2}{M^2 + Q^2} \left( 1 + \frac{2M^2}{M^2 + Q^2} \right) \xrightarrow{Q \rightarrow 0} \frac{M^2}{M^2 + Q^2} \left[ 1 - \frac{2}{3} \frac{Q^2}{M^2} \right] \\
F_{\text{eff}}[1^+] &= \sqrt{2} \left( \frac{M^2}{M^2 + Q^2} \right)^2 \left[ \frac{Q^2}{M^2} \left\{ \epsilon + \frac{Q^2}{2M^2} \right\} \right]^{1/2} \xrightarrow{Q \rightarrow 0} \frac{M^2}{M^2 + Q^2} \sqrt{2\epsilon} \frac{Q}{M} \\
F_{\text{eff}}[2^+] &= \frac{M^2}{M^2 + Q^2} \left[ \frac{Q^4 + 6M^4 + 6\epsilon M^2 Q^2}{6(M^2 + Q^2)^2} \right]^{1/2} \xrightarrow{Q \rightarrow 0} \frac{M^2}{M^2 + Q^2} \left[ 1 - \frac{2 - \epsilon}{2} \frac{Q^2}{M^2} \right] \\
F_{\text{eff}}[2^-] &= \frac{M^2}{M^2 + Q^2} .
\end{aligned} \tag{19}$$

Two features are evident. First, for  $Q$  small compared to  $M$ , all but the  $1^+$  form factors are similar to the one of pseudo-scalar mesons. Secondly, all form factors asymptotically behave as  $1/Q^2$ , but the hierarchy changes,  $Q^2 F_{\text{eff}}/M^2 \rightarrow 1, 1/3, 1, 1/\sqrt{6}, 1$ . Hence, at large  $Q^2$  we predict

$$\frac{M \sigma[e^+e^-]}{\Gamma_{\gamma\gamma}} = 1 : \frac{1}{9} : 3 : \frac{5}{6} : 5 \quad \text{for } J^P = 0^- : 0^+ : 1^+ : 2^+ : 2^- . \tag{20}$$

We close this section by comparing our results with previous calculations. We have already commented upon the pseudo-scalar case. Our covariant  $P$ -wave amplitudes agree with the  $J = 1$  amplitude of [7], the  $J = 2$  amplitude of [6], the amplitudes of [12] for all  $J$ , but disagree with the  $J = 0$  expression of [6]. For  $k_i^2 = 0$  we reproduce the  $D$ -wave result of [25]. Concerning the form factors, we are not aware of calculations of the  $0^+$  and  $2^-$  form factors. An effective form factor for the  $2^+$  state is given in [6] without quoting the value of  $\epsilon$ . We reproduce their result for (the unusual value)  $\epsilon = -1/2$ . The  $1^+$  form factors were calculated in [7]. We find identical intermediate results, (4.4) and (4.5) in [7], but the final form factors were given in the single-tag limit only, multiplied by ad hoc vector-meson-dominance form factors ( $F_\rho(Q^2) = m_\rho^2/(m_\rho^2 + Q^2)$ ); for example

$$f_{TS} = 2 \frac{2\sqrt{X}}{M^2} \frac{Q_2^2}{M^2} F^2(Q_1^2) F^2(Q_2^2) . \tag{21}$$

This result was then used by TPC/ $2\gamma$  to define a form factor  $\tilde{F}$  for single-tag  $1^+$  events

$$\tilde{F}^2 = F_\rho^2(Q_1^2) F_\rho^2(Q_2^2) \frac{Q_2^2}{M^2} \left\{ 1 + \epsilon^{-1} \frac{Q_2^2}{2M^2} \right\} . \tag{22}$$

Our result for this form factor is

$$\begin{aligned}
\tilde{F}^2 &\equiv \frac{\epsilon}{2} \kappa \left( f_{ST} + \epsilon^{-1} f_{TT} \right) \\
&= \left( \frac{M^2}{2\nu} \right)^4 \left\{ \frac{Q_2^2}{M^2} \left( \frac{\nu + Q_1^2}{\sqrt{X}} \right)^2 + \epsilon^{-1} \frac{(Q_1^2 - Q_2^2)^2}{2M^4} \frac{\nu^2}{X} \right\} \\
&\xrightarrow{Q_1 \ll Q_2} \left( \frac{M^2}{2\nu} \right)^4 \frac{Q_2^2}{M^2} \left\{ 1 + \epsilon^{-1} \frac{Q_2^2}{2M^2} \right\} .
\end{aligned} \tag{23}$$

The  $(M^2/\nu)^4$  factor is in fact crucial to obtain a sensible behaviour at large  $Q_2^2$ , in contrast to (22), which approaches a constant as  $Q_2 \rightarrow \infty$ .

$i \setminus j$	$I = 1$	$I = 0$	$(I = 0)'$	$c\bar{c}$	$b\bar{b}$	$c\bar{c} [Q_2^2 < 0.1 \text{ GeV}^2]$
$0^-(1S)$	2.9	1.7	3.9	0.12	$0.13/10^3$	0.10
$0^+$	2.9	0.42	2.0	0.024	$0.99/10^5$	0.020
$1^+$	0.060	0.14	$0.35/10^2$	$0.96/10^3$	$0.43/10^6$	$0.38/10^3$
$2^+$	1.1	3.7	0.085	0.012	$0.85/10^5$	$0.98/10^2$
$2^-$	0.69	0.23	1.8	$0.31/10^3$	$0.81/10^7$	$0.26/10^3$
$0^-(2S)$	1.7	0.56	4.4	0.029	$0.47/10^4$	0.024

Table 5: Cross sections for  $e^+e^- \rightarrow R[J^P]$  in nb for  $E_b = 91.25 \text{ GeV}$ ; no-tag columns 2–5, single anti-tag last column.

## 4 Cross-section results

Numerical results for a representative LEP energy are given in Table 5, appropriate for a no-tag setup, i.e. no cuts have been applied to the scattered leptons. Most event rates are sizeable, although experimental acceptance and tagging efficiency will somewhat lower the total rates [26]. In particular we find rates of about 1 pb for the  $\chi_{c1}$ , 0.1 pb for the  $\eta_b$ , and 0.03 nb for the  $\eta_c(2S)$ .

The single- $Q^2$  distribution of charmonium production is shown in Fig. 1,  $d\sigma/dQ_1^2$ . Here we have integrated over all  $Q_2$ . All distributions are steeply falling with  $Q_1^2$ , even for the  $\chi_{c1}$ . Hence the modulation of the  $Q_i$  dependence of the luminosity functions (mainly due to the  $1/Q_i^2$  photon propagator) by the form factors is rather weak. This is more clearly seen in Fig. 2, where we show ratios of  $e^+e^-$  cross sections as functions of  $Q_1^2$ , taking as reference the  $\eta_c$  distribution. This behaviour was anticipated in (19): for  $Q \ll M$ , the effective single-tag form factors all resemble that of the pseudo-scalar meson.

The situation is quite different for  $Q \gg M$ , accessible through studies of light mesons (Fig. 2). In fact, the cross-section ratios approach the asymptotic values (20) already at  $Q_1^2 \approx 5 \text{ GeV}^2$ , for example,  $d\sigma[f_1]/d\sigma[\eta] \sim 10$  and  $d\sigma[f_0]/d\sigma[\eta] \sim 0.1$ .

In Fig. 3 we compare  $\chi_{c1}$  production with  $\chi_{c2}$  production. Tensor mesons are dominated by phase-space regions where both photon virtualities  $Q_i$  are small. On the other hand, this region is suppressed for axial-vector mesons. However, this difference is pronounced only at very low  $Q^2$ , visible on logarithmic scales  $d^2\sigma/d\log_{10} Q_1^2 d\log_{10} Q_2^2$  (Fig. 3). For example,  $Q_1^2 = 10^{-1} \text{ GeV}^2$  is large enough to reach very small  $Q_2$  values. Hence the single- $Q^2$  distribution is still peaked at low  $Q^2$ .

In particular it follows that an anti-tag cut, say  $Q_2^2 < 0.1 \text{ GeV}^2$ , is no means to enrich  $1^+$  states in  $2\gamma$  event samples. In fact, the upper  $Q_2$  cut has a stronger effect on the  $1^+$  than on the  $2^+$  mesons, see Fig. 4. This can be seen also in Table 5, where in the last column we quote charmonium rates after applying an upper limit of  $0.1 \text{ GeV}^2$  on  $Q_2^2$ . Hence it appears sensible to search for  $1^+$  mesons also in no-tag event samples and/or single-tag samples where no anti-tag is applied to the other electron.

Since we feel that the  $Q^2$  behaviour of  $1^+$  mesons is not yet fully appreciated, we want to exhibit its  $Q^2$  dependence also analytically. For studies of the low- $Q_i$  behaviour of  $2\gamma$

processes in  $e^+e^-$  collisions it is convenient to consider the approximation of keeping only the leading  $Q_i$  dependences (Weizsäcker–Williams or equivalent-photon approximation). Then the luminosity functions simplify to<sup>7</sup>

$$\mathcal{L}_{A,B} \left( \prod_i \frac{d^3\mathbf{p}_i}{E_i} \right) = \left( \frac{\alpha}{2\pi} \right)^2 \frac{2\sqrt{X}}{W^2} \frac{dQ_1^2}{Q_1^2} \frac{dQ_2^2}{Q_2^2} \frac{dx_1}{x_1} \frac{dx_2}{x_2} Y_A(x_1) Y_B(x_2), \quad (24)$$

where

$$Y_T(x) = \frac{2(1-x)(1-Q_{\min}^2/Q^2) + x^2}{x}, \quad Y_S(x) = \frac{2(1-x)}{x}. \quad (25)$$

Hence the  $e^+e^-$  cross section must not vanish at low  $Q_i$  even if the two-photon cross section vanishes for  $Q_i \rightarrow 0$ : multiplying (24) by  $\sigma_{TS}$  and  $\sigma_{ST}$ , the dominant behaviour at low  $Q_i$  of the  $1^+$  cross section is

$$\sigma_{ee} = \int dQ_1^2 \int \frac{dQ_2^2}{Q_2^2} c_{ST} + \int \frac{dQ_1^2}{Q_1^2} \int dQ_2^2 c_{TS} + \dots \quad (26)$$

In fact,  $d\sigma_{ee}[1^+]/dQ_1$  is even peaked at low  $Q_1$ .

## References

- [1] S.J. Brodsky and G.P. Lepage, Phys. Rev. **D22** (1980) 2157; *ibid.* **D24** (1981) 1808.
- [2] S.J. Brodsky, C.-R. Ji, A. Pang and D.G. Robertson, SLAC-PUB-7473, May 1997, hep-ph/9705221;  
P. Kroll and M. Raulfs, Phys. Lett. **B387** (1996) 848;  
S. Ong, Phys. Rev. **D52** (1995) 3111;  
A.V. Radyushkin and R. Ruskov, JLAB-THY-97-24, June 1997, hep-ph/9706518;  
A. Anselm et al., HUTP-95/A037, November 1995, hep-ph/9603444.
- [3] Th. Feldmann and P. Kroll, Univ. of Wuppertal preprint WUB-97-18, May 1997, hep-ph/9706224.
- [4] For recent reviews see, for example, S.J. Brodsky, SLAC-PUB-7604, July 1997, hep-ph/9708345;  
G. Sterman and P. Stoler, ITP-SB-97-49, August 1997, hep-ph/9708370.
- [5] G. Köpp, T.F. Walsh and P. Zerwas, Nucl. Phys. **B70** (1974) 461
- [6] H. Krasemann and J.A.M. Vermaseren, Nucl. Phys. **B184** (1981) 269.
- [7] R.N. Cahn, Phys. Rev. **D35** (1987) 3342; *ibid.* **D37** (1988) 833.
- [8] M. Poppe, J. Mod. Phys. **A1** (1986) 545.
- [9] D. Morgan et al., J. Phys. G: Nucl. Part. Phys. **20** (1994) A1.
- [10] G.A. Schuler, CERN-TH/96-313, hep-ph/9611249, Comput. Phys. Commun. in press.

---

<sup>7</sup> We stress that for our numerical results we keep the full dependence on  $Q_i$ , in which case the  $\mathcal{L}_{AB}$  do not factor into products of  $Q_1$ -dependent and  $Q_2$ -dependent functions.

- [11] G.T. Bodwin, E. Braaten and G.P. Lepage, Phys. Rev. **D51** (1995) 1125.
- [12] J.H. Kühn, J. Kaplan and E.G.O. Safiani, Nucl. Phys. **B157** (1979) 125.
- [13] V.A. Novikov et al., Phys. Rep. **41** (1978) 1.
- [14] TPC/2 $\gamma$  collab., H. Aihara et al., Phys. Rev. **D38** (1988) 1.
- [15] E.J. Eichten and C. Quigg, Phys. Rev. **D52** (1995) 1726.
- [16] Review of Particle Physics, Phys. Rev. **D54** (1996) 1.
- [17] E.S. Ackleh and T. Barnes, Phys. Rev. **D45** (1992) 232;  
C. Hayne and N. Isgur, Phys. Rev. **D25** (1982) 1944.
- [18] S. Godfrey and N. Isgur, Phys. Rev. **D32** (1985) 189.
- [19] C.R. Münz, Nucl. Phys. **A609** (1996) 364;  
J.D. Anderson et al., Phys. Rev. **D43** (1991) 2094.
- [20] V.M. Budnev et al., Phys. Rep. **15** (1975) 181.
- [21] CLEO collab., J. Gronberg et al., preprint CLNS 97/1477, July 1997.
- [22] S.J. Brodsky and G.R. Farrar, Phys. Rev. **D11** (1975) 1309.
- [23] V.A. Novikov et al., Nucl. Phys. **B237** (1984) 525;  
P. Kessler and S. Ong, Phys. Rev. **D48** (1993) 2974.
- [24] L. Houra-Yaou, P. Kessler, J. Parisi, F. Murgia and J. Hansson, LPC-96-53, November 1996, hep-ph/9611337.
- [25] P. Cho and M.B. Wise, Phys. Rev. **D51** (1995) 3352.
- [26] P. Aurenche, G.A. Schuler (Conveners),  $\gamma\gamma$  Physics, in Proc. Workshop on Physics at LEP2, eds. G. Altarelli et al. (CERN 96-01, Geneva, 1996), Vol. 1, p. 291.

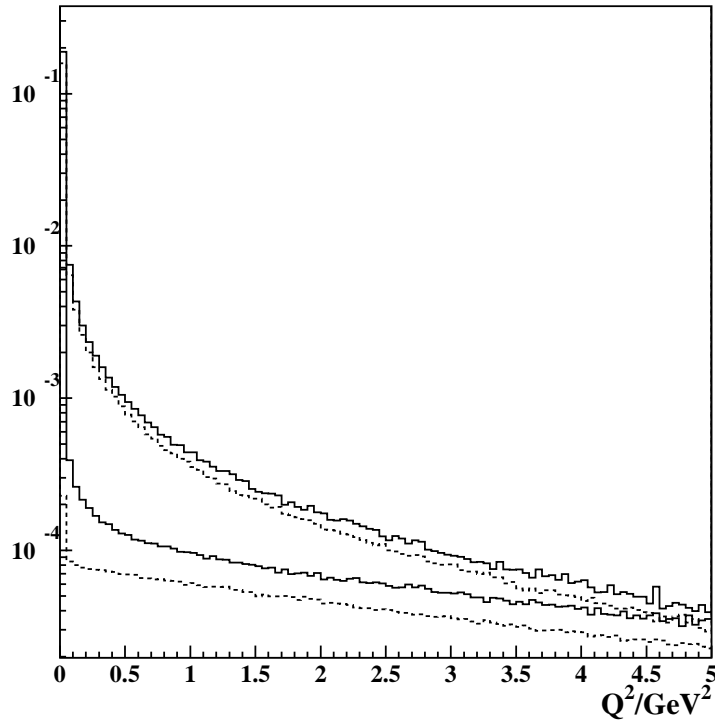
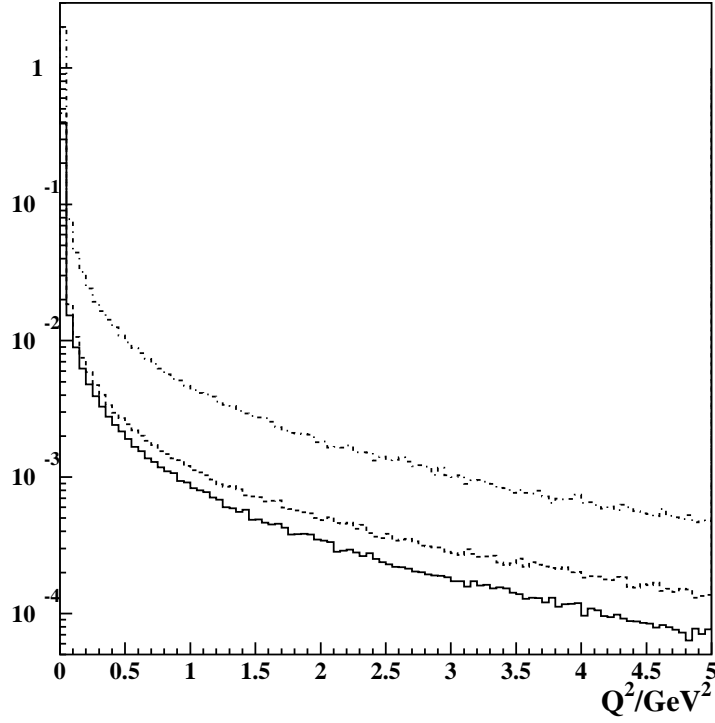


Figure 1: Top: Cross section  $d\sigma/dQ_1^2[e^+e^- \rightarrow e^+e^- M]$  in nb/GeV at  $\sqrt{s} = 92.5$  GeV for  $\eta_c(1S)$  (dash-dotted),  $\eta_c(2S)$  (dashed), and  $\chi_{c0}$  (solid). Bottom: Ditto but for  $\chi_{c2}$  (upper lines) and  $\chi_{c1}$  (lower lines); dashed lines for  $Q_2^2 < 0.1$  GeV<sup>2</sup>.

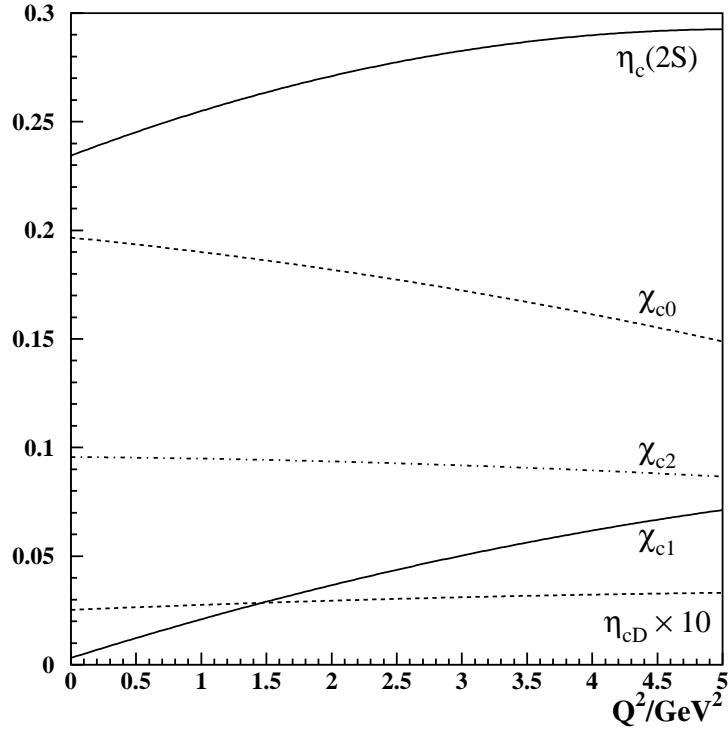
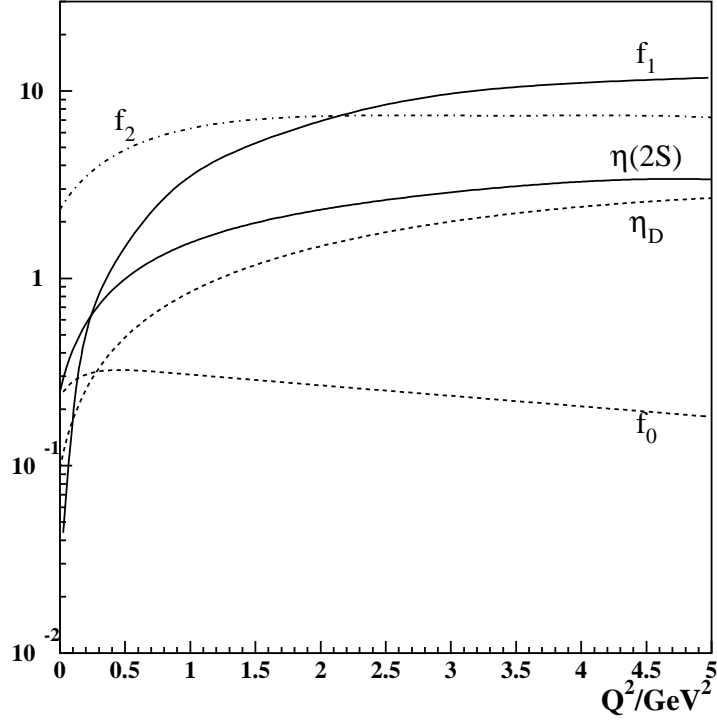


Figure 2: Cross-section ratios  $d\sigma[J^P]/dQ_1^2$  over  $d\sigma[0^-(1S)]/dQ_1^2$  in  $e^+e^- \rightarrow e^+e^- M(J^P)$  at  $\sqrt{s} = 92.5 \text{ GeV}$  for the  $\eta$  family (top) and the  $\eta_c$  family (bottom). The  $\eta_{cD}/\eta_c(1S)$  ratio is multiplied by 10.

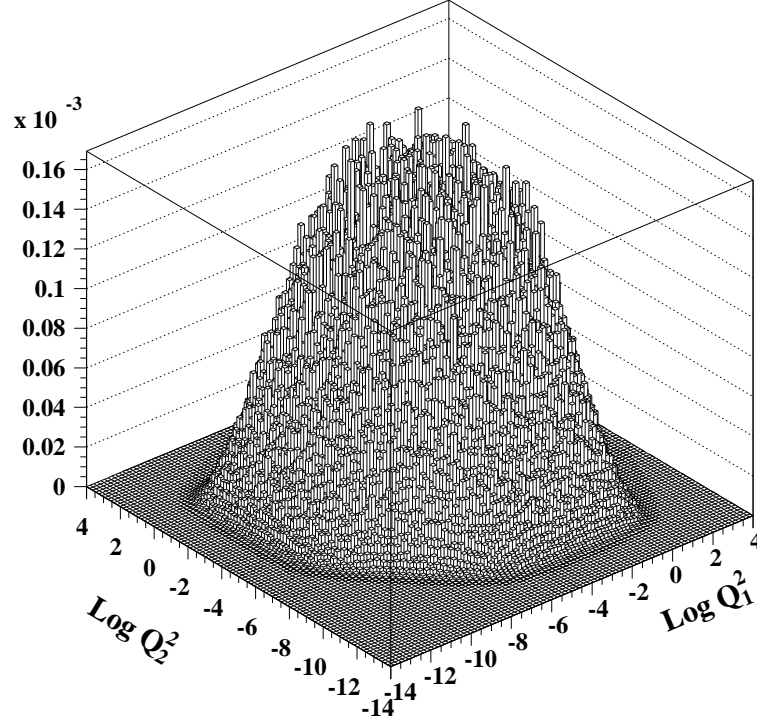
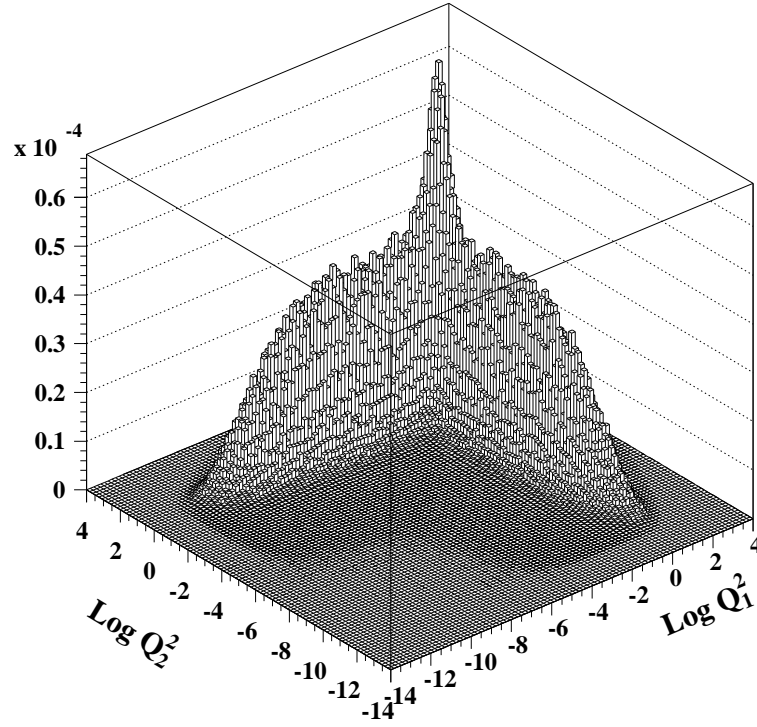


Figure 3: Cross-section  $d^2\sigma/d\log_{10}(Q_1^2/\text{GeV}^2) d\log_{10}(Q_2^2/\text{GeV}^2)$  in nb of  $e^+e^- \rightarrow e^+e^- \chi_{cJ}$  at  $\sqrt{s} = 92.5 \text{ GeV}$  for  $J = 1$  (top) and  $J = 2$  (bottom).



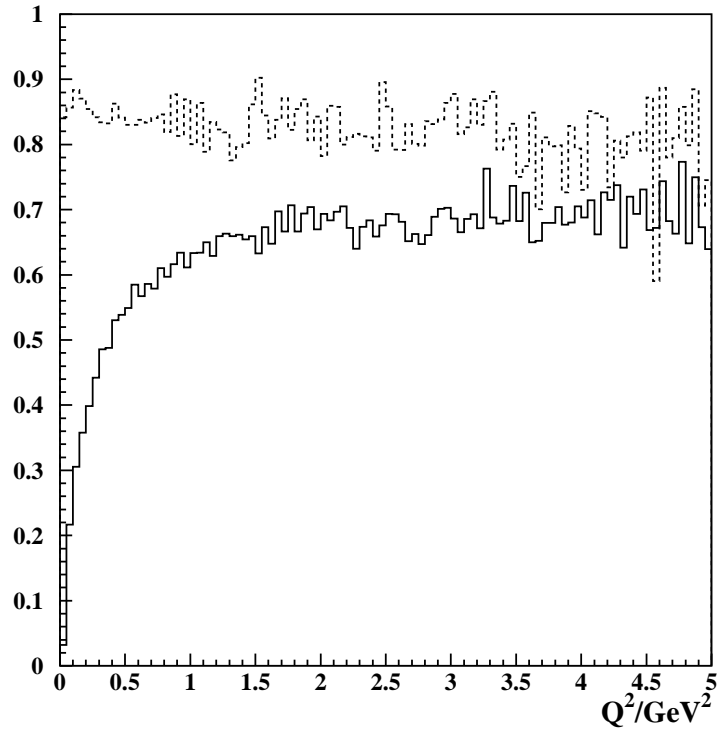
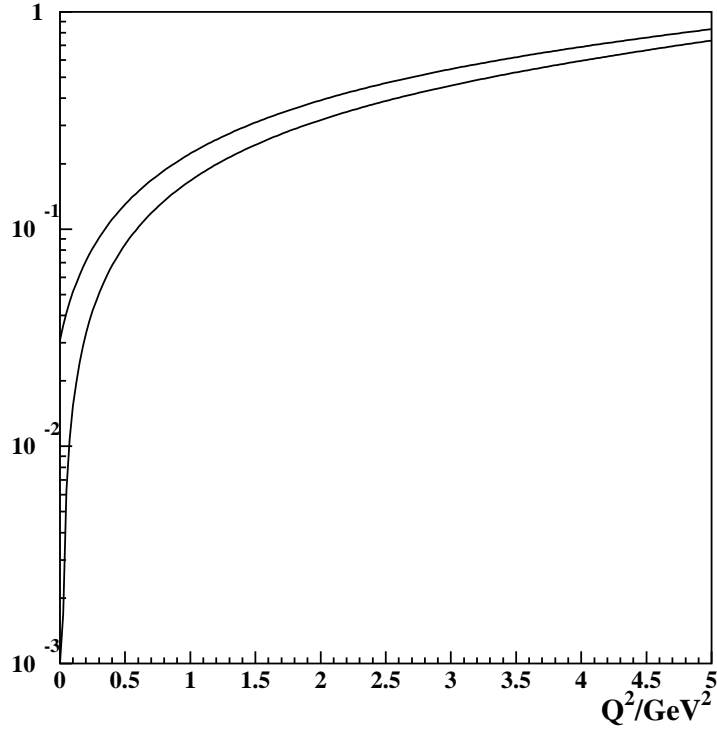


Figure 4: Cross-section ratios in  $e^+e^- \rightarrow e^+e^- \chi_{cJ}$  at  $\sqrt{s} = 92.5$  GeV. Top:  $\chi_{c1}/\chi_{c2}$  with  $Q_2^2 < 0.1$  GeV $^2$  cut (lower line) and without  $Q_2^2$  cut (upper line). Bottom:  $\chi_{c2} [Q_2^2 < 0.1$  GeV $^2]/\chi_{c2}$  [no cut] (dashed) and  $\chi_{c1} [Q_2^2 < 0.1$  GeV $^2]/\chi_{c1}$  [no cut] (solid).